

## Cold-Field Switching in PVDF-TrFE Ferroelectric Polymer Nanomesas

Igor Stolichnov,<sup>1,\*</sup> Peter Maksymovych,<sup>2</sup> Evgeny Mikheev,<sup>1</sup> Sergei V. Kalinin,<sup>2</sup>  
Alexander K. Tagantsev,<sup>1</sup> and Nava Setter<sup>1</sup>

<sup>1</sup>*Ceramics Laboratory, EPFL-Swiss Federal Institute of Technology, Lausanne 1015, Switzerland*

<sup>2</sup>*Center for Nanophase Materials Sciences, Oak Ridge National Laboratory, Oak Ridge, Tennessee, 37831, USA*

(Received 7 July 2011; published 11 January 2012)

Polarization reversal in ferroelectric nanomesas of polyvinylidene fluoride with trifluoroethylene has been probed by ultrahigh vacuum piezoresponse force microscopy in a wide temperature range from 89 to 326 K. In dramatic contrast to the macroscopic data, the piezoresponse force microscopy local switching was nonthermally activated and, at the same time, occurring at electric fields significantly lower than the intrinsic switching threshold. A “cold-field” defect-mediated extrinsic switching is shown to be an adequate scenario describing this peculiar switching behavior. The extrinsic character of the observed polarization reversal suggests that there is no fundamental bar for lowering the coercive field in ferroelectric polymer nanostructures, which is of importance for their applications in functional electronics.

DOI: [10.1103/PhysRevLett.108.027603](https://doi.org/10.1103/PhysRevLett.108.027603)

PACS numbers: 77.80.Fm, 77.55.-g, 77.84.Jd, 85.50.Gk

Ferroelectric polymers, in particular, polyvinylidene fluoride (PVDF) and its copolymers, offer an attractive combination of properties such as relatively high spontaneous polarization, piezoelectricity, electrical strength, chemically inert behavior, and durability. These benefits together with benign processing demands explain the attention that polyvinylidene fluoride with trifluoroethylene (PVDF-TrFE) thin films receive, in particular, for non-volatile memories and full-organic transistors [1–5]. Beyond conventional memory applications, PVDF-TrFE layers can be integrated on a wide range of semiconductor systems enabling novel device functionalities. A spectacular example of this approach is the organic photovoltaic device with the charge separation enhanced by a ferroelectric polymer layer [6]. Another example from the field of multiferroics is the field-effect device where the ferromagnetism in a thin diluted magnetic semiconductor layer is controlled via the persistent field effect of the PVDF-TrFE ferroelectric gate [7].

Apart from the practical interest for functional electronics, PVDF-TrFE represents a useful model system for exploring fundamentals of ferroelectricity. A unique combination of a low dielectric constant and high spontaneous polarization results in a relatively weak depolarization effect, which permits us to readily probe ferroelectricity in ultrathin films with a thickness of a few monolayers, close to the fundamental limit of ferroelectricity. A peculiar switching behavior of ultrathin PVDF-TrFE films characterized by intrinsic switching kinetics has been reported [8], whereas thicker films show conventional extrinsic switching with thermally activated dependence [9]. The differentiation between the intrinsic (reaching the spinodal on the temperature-electric field phase diagram) and extrinsic switching has been addressed in Refs. [8,10] focused on polarization reversal analysis in PVDF-TrFE.

Customarily, by using the term “extrinsic switching” one implies the switching driven by nucleation of reverse domains assisted by thermal fluctuations and the subsequent domain wall motion. However, there exists a particular kind of extrinsic switching that is promoted by the defects of the material rather than by these fluctuations. In this scenario, the nucleolus of the reverse domain located at a defect becomes unstable when the electric field exceeds a certain threshold value. In other words, this mode of switching behavior occurs when the external electric field is high enough to completely suppress the potential barrier for the polarization domain nucleation [11]. This special case of extrinsic switching that we call after Ref. [11] “cold-field switching” may look very similar to the true intrinsic switching, since in both cases the typical activation dependence of thermally activated switching is absent. However, the difference between these two switching regimes is quite profound and can be of practical importance for PVDF and other systems with high coercive fields. Indeed, the intrinsic switching does not require any nucleation at all, whereas the cold-field switching is still a nucleation-triggered process. Hence, in the case of cold-field switching the polarization reversal can be, in principle, enhanced via lowering the nucleation barrier by modifying the interface of the ferroelectric film and/or adding dopants, etc. This approach is of practical interest for PVDF-TrFE films known for very high coercive voltage  $V_C$  representing a significant drawback for potential electronic applications.

Here we explore switching in PVDF mesas in the scanning probe tip geometry in a wide temperature range and show that it is most adequately described by the cold-field switching mechanism. For this study 77/23 PVDF-TrFE mesas with a high degree of crystallinity have been prepared on Au-coated silicon substrate by spin coating using

a 0.25% methyl ethyl ketone solution deposited at 2000 rpm. After annealing at 137 °C/10 min, the thin polymer layer transforms into mesas with a lateral size of 100–300 nm and a height of 40–50 nm [Fig. 1(a)]. In addition to the ferroelectric mesas, thin film capacitors with a thickness of 100 nm have been fabricated for reference purposes. For these capacitors we used a 2% solution fabricated from the same precursors, same substrate, and annealing profile as for nanomesas, and 50 nm Au top electrodes with an area of  $3.2 \times 10^{-3} \text{ cm}^2$  have been deposited by thermal evaporation. X-ray  $\theta$ - $2\theta$  scans performed on our PVDF-TrFE samples show clear peaks at  $19.7^\circ$ , which corresponds to (110)  $d$  spacing of the all-trans ferroelectric  $\beta$  phase. The high degree of crystallinity was further proved by measurements of saturating piezoelectric loops and sharp polarization hysteresis loops with the

spontaneous polarization close to the maximal expected value (Ref. [12] provides further details).

Polarization switching has been investigated at the temperature range from 89 to 326 K under ultrahigh vacuum  $< 1E - 9$  Torr by using a commercial (Omicron) variable temperature scanning probe microscope modified for piezoresponse force microscopy.

Because of the complicated nature of charge transfer in PVDF-based polymers, discrimination between the true ferroelectric switching and contributions due to the electret effects and dielectric relaxation may present additional difficulties. In order to avoid potential problems with obtaining accurate values of coercive voltages, surface strain due to the applied dc electric field was directly measured instead of the conventional low signal piezoelectric response. In the strain curves representing the vertical

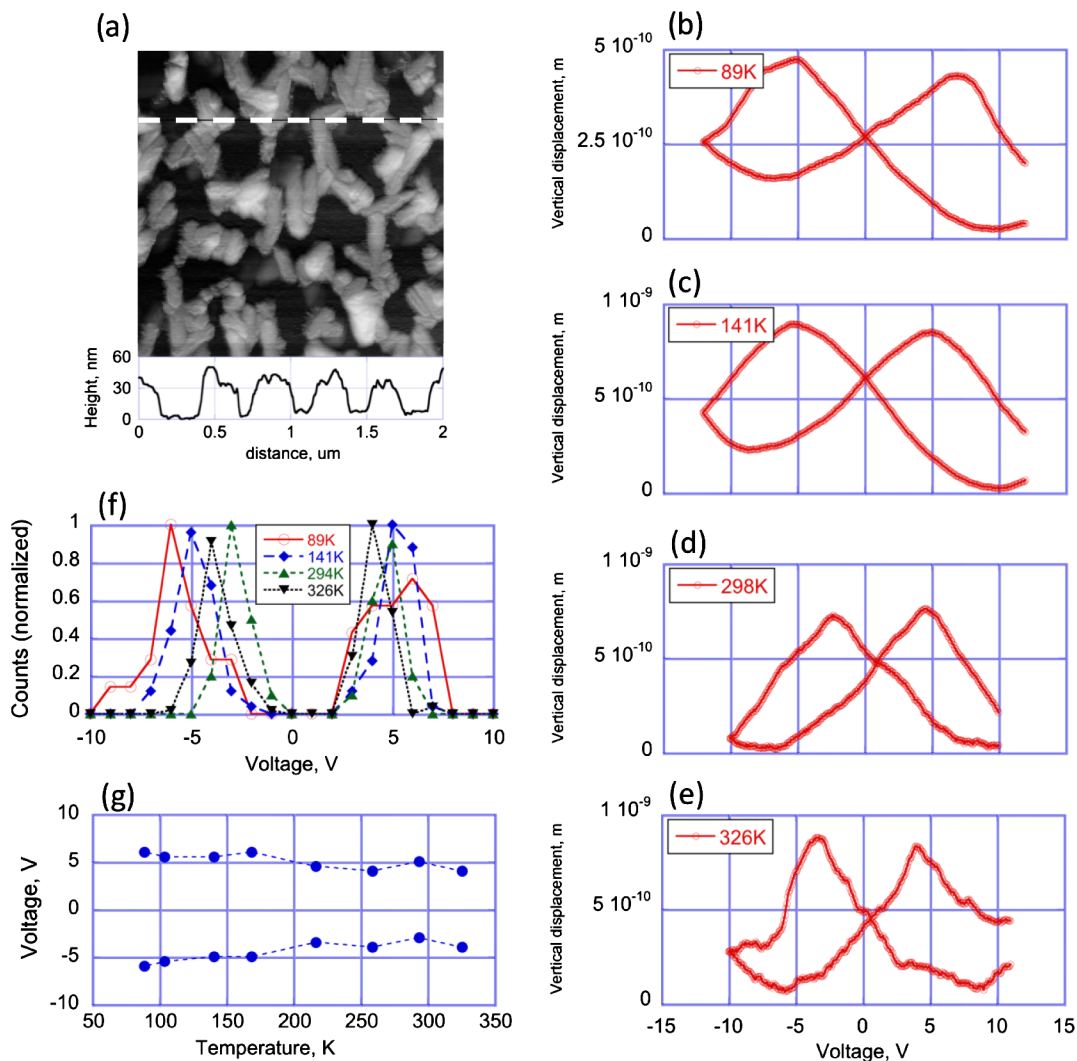


FIG. 1 (color online). (a) Topography image of PVDF-TrFE mesas deposited on the Au-coated silicon wafer and height profile measured along the dashed line. (b)–(e) Vertical displacement of the PFM cantilever vs applied voltage (strain curves) measured on PVDF-TrFE mesas at 89, 141, 298, and 326 K. The smoothness of the raw curves plotted as measured without any averaging attests to a good stability and low noise in this measurement. (f) Distributions of coercive voltage measured on 20–50 different spots at each temperature, for 89, 141, 298, and 326 K. (g) Coercive voltage extracted from the strain curve maxima vs temperature.

displacement of the cantilever as a function of bias, the coercive voltage  $V_C$  is signaled by a maximum (or minimum) around the piezoelectric coercive field.

Figures 1(b)–1(e) show typical strain curves measured at 89–326 K with a triangular voltage wave with the period of 2 s. Because of the negative longitudinal piezoelectric coefficient  $d_{33}$ , the curve tips point downwards while  $V_C$  corresponds to the maximum unlike the common ferroelectric perovskites. The strain curve maxima uniquely identify the ferroelectric switching process in PVDF-TrFE as opposed to extrinsic processes related to charge injection or surface damage (which would be, in general, manifested as topographic changes). The quality of the single strain curves allowed us to eliminate multiple loop collection with subsequent averaging, to avoid charge accumulation and electret memory effects that may influence  $V_C$  measurements. The single unprocessed strain loops shown in Figs. 1(b)–1(e) illustrate a very high stability and low noise in this measurement.

The strain loops have been previously measured on PVDF-TrFE layers by using parallel-plate capacitor geometry via the interferometer technique [13] and a scanning tunneling microscope [14]. Both groups reported loops with an abrupt change of strain near the coercive field. Compared to these data, the strain loops in Fig. 1(b)–1(e) are much smoother and characterized by rounded peaks close to  $V_C$ . This difference is linked to the geometry of our experiment, where the piezoelectric properties are probed by the piezoresponse force microscopy (PFM) tip, which serves as a top electrode. This technique provides very selective local switching within the region comparable with the tip radius (as opposed to the entire capacitor switching in Refs. [13,14]). On the other hand, the difficulty associated with this local probing technique is a nonuniform electric field, and consequently the switching characteristics are never as sharp as in the capacitor configuration.

The magnitude of measured strain proves that the complete polarization reversal has been achieved in the measurements shown in Figs. 1(b)–1(e). The value of transverse piezoelectric coefficient  $d_{33}$  in P(VDF-TrFE) with a composition of 78/22 (nearly the same composition as our material) quoted in Ref. [13] is 40 pm/V. Hence, the application of 10 V to the completely poled film results in a displacement of 4 Å. This is very close to our room temperature data from Fig. 1, where 5 Å displacement corresponds to the voltage change from 0 to 10 V applied to the fully poled nanomesa. It is impossible to reach such a significant deformation by electrostriction in nonpoled or partially poled films.

The strain amplitude decrease at lower temperatures observed in Fig. 1 also agrees with the piezoelectric effect. Indeed, the transverse piezoelectric coefficient is proportional to both the dielectric constant and polarization, both being sensitive to the temperature. However, within the studied temperature range polarization is a relatively weak

function of temperature, while the dielectric constant changes quite significantly. In our measurements performed on the reference capacitor of the dielectric constant dropped from 7.7 at 293 K to 3.5 at 90 K, i.e., by factor of 2.2 (as shown in Ref. [12]), this factor closely corresponds to the change of the amplitude of the strain curve observed in Fig. 1 at these temperatures.

A systematic study of temperature dependence of  $V_C$  has been performed by measuring strain curves on 20–50 different spots at each temperature and analyzing the distribution of  $V_C$  for 8 temperature values within the range from 89 to 326 K. Figure 1(f) representing  $V_C$  values obtained at temperatures of 89, 141, 294, and 326 K shows a slight increase and broadening distribution of  $V_C$  with the temperature decrease. The  $V_C$  data from the entire temperature range [Fig. 1(g)] attest to a weak nonactivation-type temperature dependence of the coercive field, in dramatic contrast to the strongly temperature-dependent extrinsic switching typically observed in PVDF-TrFE in this thickness range. This prompts an interpretation in terms of intrinsic switching; however, the switching data obtained for PVDF-TrFE films in the parallel-plate capacitor configuration do not agree with this scenario. Indeed, in Au/PVDF-TrFE/Au capacitors, the coercive field extracted from the conventional polarization-electric field hysteresis loops [Fig. 2(a), inset] shows nearly linear dependence on  $1/T$ , in agreement with the theory for thermally activated nucleation-controlled switching [Fig. 2(a)]. This dependence holds at least up to 6 MV/cm, indicating that the thermodynamic coercive field exceeds 6 MV/cm. On the other hand, the gold-plated cantilever tip with radius  $>50$  nm generates a maximal electric field  $<2$  MV/cm, for the bias voltage of 10 V (for details, see Refs. [12,15]). In this case, in the scanning-probe microscopy experiment the maximal electric field seen by the ferroelectric polymer is at least 3 times lower than the field of intrinsic switching. Thus the polarization reversal in nanomesas cannot be described by intrinsic switching. An adequate description of the switching process in this case is given by the cold-field switching mechanism that combines the nucleation-controlled kinetics and weak temperature dependence seen in Fig. 1(g).

The apparent discrepancy between the switching behavior of PVDF-TrFE nanomesas and capacitors needs to be separately addressed. Our interpretation relies on the following key assumptions: (i) Cold-field switching mediated by defects occurs in the nanomesas as well in capacitors; (ii) in the capacitors, the cold-field switching results in a local polarization reversal in small areas (negligible compared to the capacitor area) without triggering the entire capacitor switching. The impossibility to switch the capacitor through the cold-field mechanism is explained by the secondary (amorphous) phase existing in a small quantity even in a well-crystallized film. The inclusions of the amorphous phase between the polymer

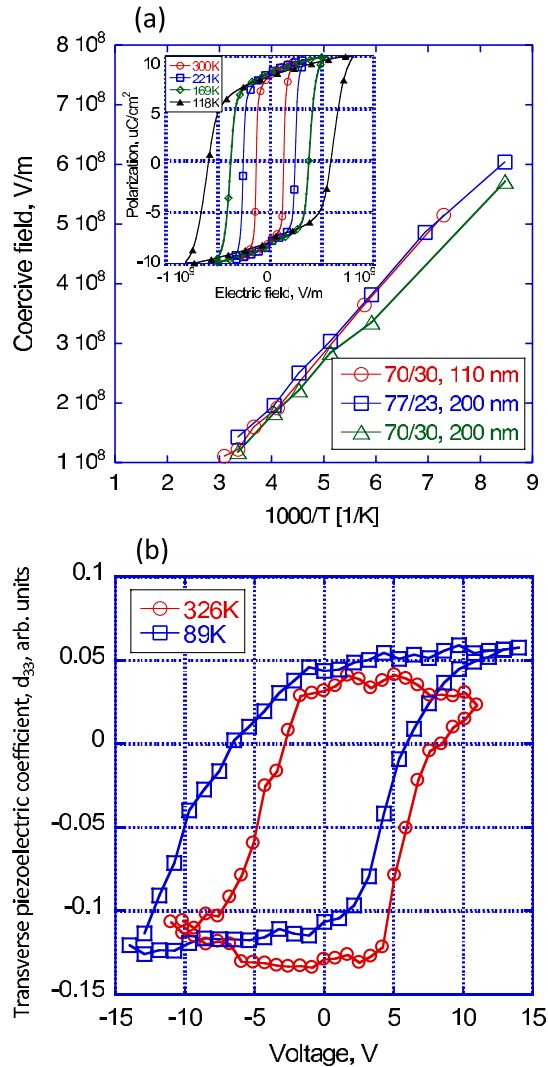


FIG. 2 (color online). (a) Macroscopic data of coercive field vs temperature extracted from polarization-voltage loops measured on Au/PVDF-TrFE/Au capacitors with different compositions and a thickness of 110 and 200 nm. Inset: Typical 10 kHz polarization-voltage hysteresis loops used for the coercive field determination. (b) Local piezoelectric hysteresis loops measured on 50 nm PVDF-TrFE mesas via the resonant band excitation technique by PFM at 326 and 89 K.

grains produce barriers, which impede switching at low temperature. In the previous work [16], we clearly observed by PFM in PVDF-TrFE capacitors some boundaries inhibiting the propagation of the switched state, which we attribute to this effect. Unlike capacitors, the nanomesas represent compact islands composed of a small number of densely packed grains where the amorphous phase inclusions are more likely to concentrate close to the boundaries or outside the main cluster of polymer grains. Hence, cold-field switching in the nanomesa results in the polarization reversal, while in the capacitor it switches only some isolated nanoscale areas, which are not noticeable when measuring the macroscopic hysteresis loops.

The shape of piezoelectric hysteresis loops is another differentiator that allows for discrimination between intrinsic switching and cold-field switching. In the case of intrinsic switching, upon approaching the thermodynamic coercive field  $E_{th}$ , the electric field drives a given domain state of the ferroelectric to lose its stability. This implies a divergence of the small signal response to electric field, specifically, an anomalously high longitudinal piezoelectric coefficient  $d_{33}$  at the coercive field which, in this scenario, equals  $E_{th}$ . In contrast, extrinsic switching occurs at fields much smaller than  $E_{th}$ , so that no singularity of  $d_{33}$  at the coercive field of the loop is expected [17]. In reality, in view of the finite amplitude of the measuring ac field, the aforementioned singularity will be smeared. However, if this amplitude is appreciably smaller than that of the ramping field of the loop, the intrinsic switching must reveal itself by a measurable increase of  $d_{33}$  on approaching the coercivity. We have employed this criterion for the analysis of our data. Figure 2(b) shows hysteresis loops of transverse piezoelectric coefficient  $d_{33}$  obtained via the resonant band excitation technique [18] at 326 and 89 K. In both cases the loops are characterized by a pronounced saturation behavior with no visible increase of  $d_{33}$  at the coercive voltage. This can be considered as an additional argument in favor of cold-field switching scenario.

Further studies are required to identify the nature of defects responsible for the cold-field switching. The defects associated with the all-trans ( $\beta$ -phase) molecular conformation and molecular packing [19] can influence the switching kinetics in PVDF-TrFE nanomesas stabilizing residuals of the opposite domains especially in the crystallite extremities. Then these residuals may serve as nucleation centers for switching in the reverse direction via the cold-field switching mechanism.

In conclusion, polarization switching characterized by a weak nonactivation-type temperature dependence has been observed in PVDF-TrFE mesas. The appealingly straightforward interpretation in terms of the intrinsic switching appears to be incompatible with the macroscopic data showing that within the studied range of electric fields the switching is purely extrinsic. An additional argument against the intrinsic switching is the piezoelectric loop shape, which does not agree with the intrinsic switching scenario. We show that the observed behavior of local polarization reversal is compatible with a particular kind of extrinsic switching promoted by the defects of the material rather than by the thermal fluctuations. In this switching mode, which occurs when the external electric field is high enough to completely suppress the domain nucleation potential barrier, the switching rate does not obey any thermally activated dependence of temperature similar to the classic intrinsic switching. However, despite this similarity, the presented switching mechanism is fundamentally different from the true intrinsic switching since it relies on the nucleation centers. The important practical



implication is a possibility to influence the switching properties via the introduction of artificial nucleation centers, e.g., by doping and chemical or mechanical modification of the polymer film interface. Hence, the high electric fields typically required to switch ferroelectric polymer films and nanostructures can be, in principle, lowered, which would make these materials even more attractive for electronic application.

We acknowledge support from the Swiss National Science Foundation. EU is acknowledged for financial support through the project ERC-268058 MOBILE-W. PFM microscopy was conducted through user project CNMS2010-094 at the Center for Nanophase Materials Sciences, which is sponsored at Oak Ridge National Laboratory by the Office of Basic Energy Sciences, U.S. Department of Energy.

---

\*igor.stolitchnov@epfl.ch

- [1] R. C. G. Naber, C. Tanase, P. W. M. Blom, G. H. Gelinck, A. W. Marsman, F. J. Touwslager, S. Setayesh, and D. M. De Leeuw, *Nature Mater.* **4**, 243 (2005).
- [2] A. Gerber, M. Fitsilis, R. Waser, T. J. Reece, E. Rije, S. Ducharme, and H. Kohlstedt, *J. Appl. Phys.* **107**, 124119 (2010).
- [3] T. Nakajima, Y. Takahashi, S. Okamura, and T. Furukawa, *Jpn. J. Appl. Phys.* **48**, 09KE04 (2009).
- [4] X. B. Lu, J. W. Yoon, and H. Ishiwara, *J. Appl. Phys.* **105**, 084101 (2009).
- [5] L. Malin, I. Stolichnov, and N. Setter, *J. Appl. Phys.* **102**, 114101 (2007).
- [6] Y. B. Yuan, T. J. Reece, P. Sharma, S. Poddar, S. Ducharme, A. Gruverman, Y. Yang, and J. S. Huang, *Nature Mater.* **10**, 296 (2011).
- [7] I. Stolichnov, S. W. E. Riester, H. J. Trodahl, N. Setter, A. W. Rushforth, K. W. Edmonds, R. P. Campion, C. T. Foxon, B. L. Gallagher, and T. Jungwirth, *Nature Mater.* **7**, 464 (2008).
- [8] G. Vizdrik, S. Ducharme, V. M. Fridkin, and S. G. Yudin, *Phys. Rev. B* **68**, 094113 (2003).
- [9] R. V. Gaynutdinov, O. A. Lysova, A. L. Tolstikhina, S. G. Yudin, V. M. Fridkin, and S. Ducharme, *Appl. Phys. Lett.* **92**, 172902 (2008).
- [10] H. Kliem and R. Tadros-Morgane, *J. Phys. D* **38**, 3554 (2005).
- [11] G. Gerra, A. K. Tagantsev, and N. Setter, *Phys. Rev. Lett.* **94**, 107602 (2005).
- [12] See Supplemental Material at <http://link.aps.org/supplemental/10.1103/PhysRevLett.108.027603> for characterization data of the ferroelectric polymer and analysis of the electric field generated by the scanning probe.
- [13] T. Furukawa and N. Seo, *Jpn. J. Appl. Phys.* **29**, 675 (1990).
- [14] L. Jie, C. Baur, B. Koslowski, and K. Dransfeld, *Physica (Amsterdam)* **204B**, 318 (1995).
- [15] M. Molotskii, *J. Appl. Phys.* **93**, 6234 (2003).
- [16] R. Gysel, I. Stolichnov, A. Tagantsev, N. Setter, and P. Mokry, *J. Appl. Phys.* **103**, 084120 (2008).
- [17] A. Tagantsev, E. Cross, and J. Fousek, *Domains in Ferroic Crystals and Thin Films* (Springer, New York, 2010).
- [18] S. Jesse, S. V. Kalinin, R. Proksch, A. P. Baddorf, and B. J. Rodriguez, *Nanotechnology* **18**, 435503 (2007).
- [19] A. Gruverman, P. Sharma, T. J. Reece, and S. Ducharme, *Nano Lett.* **11**, 1970 (2011).